Journal of Plant Biology (2021) 64:349–358
https://doi.org/10.1007/s12374-021-09308-3

RESEARCH ARTICLE

Transcriptome Analysis on Asymmetric Root Growth of *Oryza sativa* Induced by Brassinosteroids via Ethylene Pathway

Zeping Cai[1] · Zhen Huang[1] · Chujun Huang[1] · Xia Jin[1] · Wen Yang[1] · Gengbo Jiang[1] · Zixuan Wang[1] · Fanhua Wu[3] · Xudong Yu[1] · Jiajia Luo[2]

Received: 7 December 2020 / Revised: 11 February 2021 / Accepted: 2 March 2021 / Published online: 25 March 2021

Abstract

The growth of plant roots is regulated by various factors. Brassinosteroids (BRs) can induce asymmetric root growth (ARG) to form waves and coils, and this phenomenon can be eliminated by ethylene (ETH) inhibitors aminoacetic acid (AOA) or silver thiosulfate (STS), indicating this process depends on ETH pathway. Nevertheless, the research on related genes has not been reported. In this study, four treatments (Water, Brassinolide (BL), BL + AOA, and BL + STS) were set up using the seedlings of *Oryza sativa* as materials. The differentially expressed genes (DEGs) in BR-induced ARG via ETH pathway were identified by transcriptome sequencing, weighted gene co-expression network analysis (WGCNA), and real-time quantitative PCR (qRT-PCR). Finally, we screened 70 DEGs, including *ALPHA-EXPANSINs* (*OsEXPAs*), *WALL-ASSOCIATED RECEPTOR KINASE-LIKE 16* (*OsWAKL16*), and *TRANSMEMBRANE KINASE* (*OsTMK*) that regulated cell elongation and expansion, as well as plant hormone synthase genes, *1-AMINO-CYCLOPROPANE-1-CARBOXYLIC ACID OXIDASEs* (*OsACOs*), *OsYUCCAs*, and *CYTOKININ OXIDASE*(*OsCKX*). Most of them were up-regulated by BRs via ETH pathway. In addition, the receptor-like kinase (RLK) gene *ROOT MEADNDER CURLING* (*OsRMC*), a negative regulator in jasmonic acid-induced ARG, could be inhibited by BRs, and this process also depended on ETH pathway. The identification of the above genes provides evidence for revealing the molecular mechanism in the process.

Keywords Brassinosteroids · Ethylene · Asymmetric root growth · Transcriptome analysis

Zeping Cai, Zhen Huang, and Chujun Huang contributed equally to this work.

✉ Jiajia Luo
992995@hainanu.edu.cn

Zeping Cai
494266605@qq.com

Zhen Huang
2661220929@qq.com

Chujun Huang
hcjstu@163.com

Xia Jin
2390735483@qq.com

Wen Yang
1114074166@qq.com

Gengbo Jiang
1245516454@qq.com

Zixuan Wang
940518586@qq.com

Fanhua Wu
1833991632@qq.com

Xudong Yu
yxd172839@outlook.com

[1] Key Laboratory of Genetics and Germplasm Innovation of Tropical Special Forest Trees and Ornamental Plants, Ministry of Education, College of Forestry, Hainan University, Haikou 570228, P. R. China

[2] Tropical Crops Genetic Resources Institute, Chinese Academy of Tropical Agricultural Sciences, Haikou 571101, P. R. China

[3] School of Life and Pharmaceutical Sciences, Hainan University, Haikou 570228, P. R. China

Introduction

Plant roots can perceive various factors to adjust their growth patterns (types of movement) (Roy and Bassham 2014). Under gravity, roots grow downwards (Blancaflor and Masson 2003; Mori et al. 2016); while under certain conditions, they will grow asymmetrically to form waves and coils (Cai et al. 2018). As early as more than 100 years ago, Darwin (1880) had noticed that the roots had the wavy or helix phenotype when seedlings (e.g., legumes) were cultured on inclined plates (Darwin 1880). However, limited to the fact that plant hormones had not been found at that time, the phenomenon could not be explained. Okada and Shimura (1990) screened six *Arabidopsis* mutants with root-wave growth phenotype by ethyl methanesulfonate (EMS) mutagenesis. Among them, *wav5* and *wav6* were caused by the mutations of auxin influx and efflux carrier genes (*AtWAV5*/*AtAUX1* and *AtWAV6*/*AtPIN2*), respectively, showing that the changes of auxin flux and distribution in roots could lead to asymmetric root growth (ARG) (Okada and Shimura 1990; Robert et al. 2009; Roy and Bassham 2014). ETH could also induce ARG, and Buer et al. (2003) found that the spatial frequency of root waving was positively correlated with ethylene (ETH) concentration ($\leq 1\ \mu LL^{-1}$) (Buer et al. 2003). After that, the ARG regulated by jasmonic acid (JA) and brassinosteroids (BRs) were reported (Jiang et al. 2007; Mónica Lanza et al. 2012; Cai et al. 2018). Although many plant hormones played roles in the regulation of ARG, the specific mechanism and the relationship between them were still poorly understood (Roy and Bassham 2014).

BRs represent a class of polyhydroxysteroid plant hormones. So far, more than 70 natural derivatives have been found, among which brassinolide (BL) has the highest biological activity (Mandava 1988; Gudesblat and Russinov, 2011; Bajguz, 2007). BRs play important roles in plant growth and development, as well as in mediating biotic and abiotic stresses responses (Kurepin et al. 2016; Mohsin Tanveer et al. 2018; Hu et al. 2016). In BRs synthetic mutants (e.g., *det2*, *cpd*) or signaling transduction mutants (e.g., *bri1*), the elongation of root cells was inhibited, showing a short-root phenotype (Clouse et al. 1996; Jianming and Kyoung (2002); Fujioka et al. 1997; Fridman et al. 2014). In addition, BRs could also induce ARG (Cai et al. 2018; Roy and Bassham 2014). In both monocotyledonous *Oryza sativa* (*O. sativa*) and dicotyledonous *Brassica chinensis*, the ratios of ARG increased with the increase of exogenous BL concentration ($\leq 2\times10^{-7}$ M) (Cao et al. 2019; Cai et al. 2018). Besides, the lengths of the outer cells were significantly greater than those of the inner cells in coiled *O. sativa* roots (Cai et al. 2018).

ETH is a gaseous plant hormone. Exogenous application of ETH can induce the root coiling in *Lycopersicon esculentum* seedlings (Woods et al. 1984). As an analog of pyridoxal-5′- phosphate (PLP), the prosthetic group of 1-aminocyclopropane-1-carboxylic acid synthases (ACS), aminooxyacetic acid (AOA) can competitively bind to the zymoprotein and inactivate it. It is a specific inhibitor of ETH biosynthesis (Peiser et al. 1984; Spollen et al. 2000; Wang et al. 2009). Additionally, the ETH receptor has cuprous ion (Cu^+)-binding sites. Silver ion (Ag^+) can also bind to ETH after replacing Cu^+ to bind with the receptor, but it cannot mediate the signaling transduction. Moreover, Ag^+ can cause ETH inactivation through a chemical complexation reaction with ETH, demonstrating that Ag^+ is an ETH perception antagonist (Beyer 1976, 1979; Nymeijer et al. 2004). The BR-induced ARG could be eliminated by the two ETH antagonists, AOA or STS, suggesting that this process depended on ETH pathway. However, the research on related genes has not been reported yet (Cai et al. 2018).

In view of this, we used transcriptome sequencing, weighted gene co-expression network analysis (WGCNA), and real-time quantitative PCR (qRT-PCR) technologies to analyze the expression levels of all genes in the root tips of *O. sativa* under four treatments (Water, BL, BL + AOA, and BL + STS). Finally, the genes related to BR-induced ARG via ETH pathway were screened, which provided a reference for exploring its molecular mechanism.

Materials and Methods

Experimental Materials and Drugs

The *O. sativa* variety was Xiuzhan 15, an indica conventional *O. sativa* variety, which was obtained through hybrid breeding of E'feng 28 × Fengmeizhan. BL (CAS: 78821–43-9) was purchased from Solarbio company and prepared into a 1 mM mother solution with 75% ethanol and preserved at 4 ℃. It was diluted to 2×10^{-8} M with ddH_2O as the *O. sativa* culture solution. The 0.92 mM STS solution was prepared by mixing isovolumetric 1.28 mM $Na_2S_2O_3{\cdot}5$ (H_2O) and 1.84 mM $AgNO_3$, which should be freshly prepared as required. AOA (CAS: 645-88-5) was purchased from Sigma company and prepared into a 1 mM mother solution with ddH_2O and preserved at 4 ℃. It was further diluted to 0.1 mM when used.

Experimental Methods

Culture of O. sativa Seedlings and Collection of Root Tips

O. sativa seeds were sterilized and germinated according to the method of Cai et al. (2018). Four treatments (Water, 2×10^{-8} M BL, 2×10^{-8} M BL + 0.1 mM AOA, and

2×10^{-8} M BL + 0.92 mM STS) were set up. Under the conditions of 24 ℃ ± 1 ℃ and 5000 lx light intensity, 60 *O. sativa* seedlings were cultured in each petri dish (Ø 150 mm) for 24 h. Because the coiling occurred at the root tip, and it took about 5 mm to curl a circle, the root apical length collected in this study was 5 mm. About 500 root tips (about 0.5 g in weight) were collected from each treatment and stored in liquid nitrogen. Compared with the wave, the coiling phenotype was more intense. Therefore, in BL treatment, only the coiled root tips were collected. There were three biological replicates in each treatment.

Library Construction, Sequencing, and Data Analysis

The enriched mRNAs were fragmented, and the cDNA libraries were prepared by reverse transcription. The BGISEQ-500 platform was used for sequencing. The raw data with low quality, joint contamination, and high content of unknown bases were removed to obtain clean reads. After that, the clean reads were aligned to the reference genome sequence (*O. sativa* Japonica Group, GCF_001433935.1_IRGSP-1.0) by HISAT, and the standard expression level (fragments per kilobase million, FPKM) of each gene in each sample was calculated. The above steps were completed by Beijing Genomics Institute (BGI). The transcriptome sequencing data have been uploaded to the SRA database of NCBI with the accession number of SRP278550. The Pearson correlation coefficients among samples and the principal component analysis of each sample were calculated by the cor and prcomp functions in R software, respectively.

Screening of Differentially Expressed Genes

Differentially expressed genes (DEGs) analysis was conducted by BGI using the DEGseq software (Wang et al. 2010). Low-abundance genes, whose average FPKM in each sample ≤ 0.5, were removed. And the genes were defined as DEGs when both the criteria ($|\log_2$fold change $|\geq 1$ and Q value ≤ 0.001) were satisfied.

Weighted Gene Co-expression Network Analysis

According to the method of Langfelder et al. (Langfelder and Horvath 2008), the WGCNA package in the R software was used to analyze the selected DEGs (sft$powerEstimate = 15, mergeCutHeight = 0.25). The gene module with the highest phenotypic correlation was selected for follow-up analysis.

Gene Ontology Functional Classification and Enrichment

DEGs were classified according to the Gene Ontology (GO) annotations. The Phyper package in R software was used for enrichment analysis. The P values were calculated, and the Q values were obtained after FDR correction of the P values. Generally, the Go term with a Q value ≤ 0.05 was regarded as significant enrichment.

Visualization of Gene Co-expression Network

According to the method of Michael Kohl et al. (2011), the co-expression network visualization of module genes was performed by using Cytoscape software. In the visualization graph, nodes represent genes. The higher the degree of gene connectivity, the larger the node; edges represent the weights of co-expression among genes. The larger the weight, the thicker the line and the darker the color.

qRT-PCR Verification

12 genes (Os01g0580500, Novel_G000655, Os06g0181700, Os04g0399800, Os03g0182800, Os09g0471200, Os11g0691240, Os01g0634600, Os04g0659300, Os03g0162000, Os07g0437000, Novel_G000294) were selected for performing qRT-PCR verification. The primers were synthesized by BGI (Table S1). The reactions were carried out on ABI ViiA 7 PCR machine. The PCR reaction system was 16 µl. Three parallel tests were performed on each sample. *OsACTIN* (Os03g0836000) was used as the reference gene. The $2^{-\Delta\Delta Ct}$ method was used for relative quantification (Pfaffl 2001).

Results

BR-Induced ARG of *O. sativa* Depended on ETH Pathway

In this study, four treatments (Water, BL, BL + AOA, and BL + STS) were set up at 24℃. The ARG was induced to form coiling only in the BL treatment (Fig. S1 B), and the ratios of root coiling increased with the increase of culture time (Fig. S1 E). In the other three treatments, the coiling ratios were very low or 0 (Fig. S1 A, C, D, E). Meanwhile, the AOA treatment had the strongest inhibitory effect on root length (Fig. S1 F). The above phenotypes were consistent with our previous results (Cai et al. 2018).

Evaluation of Transcriptome Sequencing Data

There were 3 biological replicates in each of the 4 treatments and 12 samples in total. Transcriptome sequencing was performed on the BGISEQ-500 platform. Each sample produced at least 6.76 Gb data, with an average output of 7.15 Gb (Table S2). Sequencing saturation analysis showed that the slopes of all curves tended to 0 when the reads number (× 100 K) > 200, indicating that the sequencing data

reached saturation (Fig. S2A). After filtering the raw reads, the amounts of clean reads were all greater than 82.3%, wherein the Q20 > 95.8% and the Q30 > 86.8%. The average rates of alignment to the reference genome and gene set were 87.15% and 76.78%, respectively. And 67.60–69.83% of the clean reads were mapped to the unique gene locus. The results indicated that the mapping rates were high (Table S2).

Cluster analysis and correlation analysis were performed on all samples according to the gene expression data (Table S3). The results showed that the three biological replicates of each treatment were clustered into one branch (Fig. S2 B), and the Pearson correlation coefficients between samples in each treatment were all greater than 0.91 (Fig. 1a). Principal component analysis (PCA) showed that BL + AOA was discrete from the other three treatments on PCA 1. While Water, BL, and BL + STS were discrete in pairs on PCA 3 (Fig. 1b). In conclusion, the 12 samples were of high quality with reliable sequencing data, which could be further analyzed.

Screening of Genes that Regulated by BL via ETH Pathway

There were 285 DEGs overlapped in the 3 pairwise comparisons (Water vs. BL, BL vs. BL + AOA, and BL vs. BL + STS) (Fig. 2a). Among them, 65 DEGs were in accordance with Log_2FC (Water vs. BL) > 1, Log_2FC (BL vs. AOA + BL) < −1, and Log_2FC (BL vs. BL + STS) < −1; 140 DEGs were in accordance with Log_2FC (Water vs. BL) < −1, Log_2FC (BL vs. BL + AOA) > 1, and Log_2FC (BL vs. BL + STS) > 1. The sum was 205, accounting for 71.93% of the total number (Fig. 2b and Table S4). WGCNA was conducted on these 205 DEGs, and 4 modules (blue, brown, turquoise, and grey) were obtained by clustering (grey includes DEGs not categorized into any module), in which the blue module had the highest phenotypic correlation and smallest *P* value (Figs. 2c, 3d; Fig. S3 and Table S6).

This module had 70 DEGs, in which the relative expressions of 60 DEGs (85.71%) were in accordance with Log_2FC (Water vs. BL) > 1, Log_2FC (BL vs. BL + AOA) < −1, and Log_2FC (BL vs. BL + STS) < −1, and only 10 DEGs (14.29%) were in accordance with Log_2FC (Water vs. BL) < −1, Log_2FC (BL vs. BL + AOA) > 1, and Log_2FC (BL vs. BL + STS) > 1. Therefore, the DEGs in the blue module were what we need. Most of them were up-regulated by BL, which depended on ETH pathway.

Gene Ontology Analysis of Module Genes

The 70 DEGs in the blue module were aligned to the GO database, among which 43 were annotated, accounting for 61.43% (Table S7). A total of 24 GO terms were annotated, included in the biological process (BP), cellular component (CC), and molecular function (MF). In the BP, most DEGs were annotated to the "cellular process" and "metabolic process". In the CC, lots of DEGs were classified to the "cell", "membrane", and "extracellular region". In the MF, most DEGs were grouped into the "catalytic activity" and "binding" (Fig. 3 and Table S7).

GO enrichment analysis was performed on 70 DEGs. 8 GO terms with the highly significant *Q*-value were:

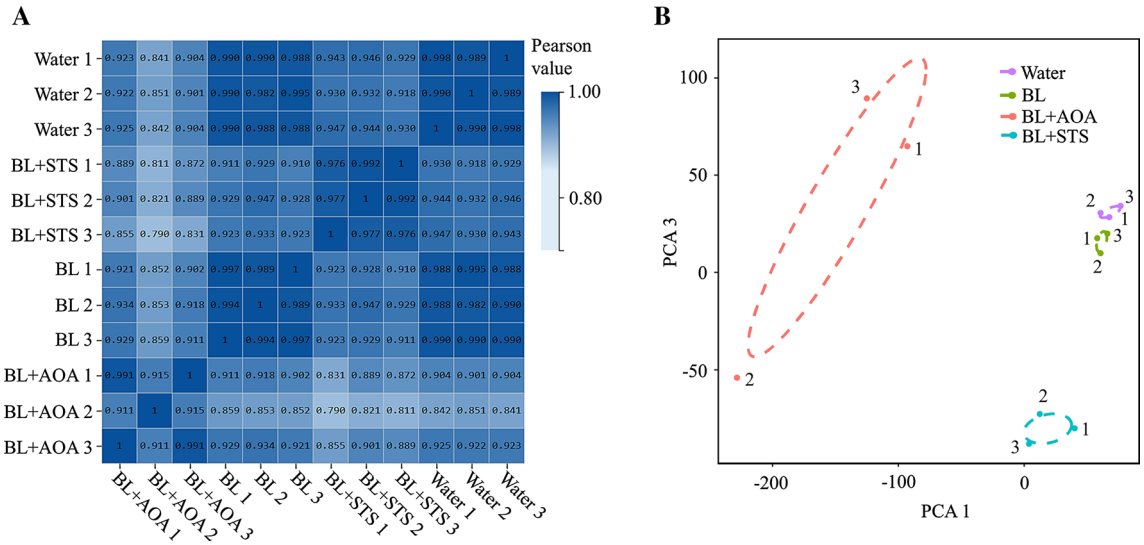

Fig. 1 Correlation among all samples of four treatments. **a**, **b** Pearson correlation coefficient analysis (**a**) and Principal component analysis (PCA) (**b**) were performed among 12 samples of four treatments using the expression data; PCA plot shows the separation of each treatment on the PCA1 and the PCA3

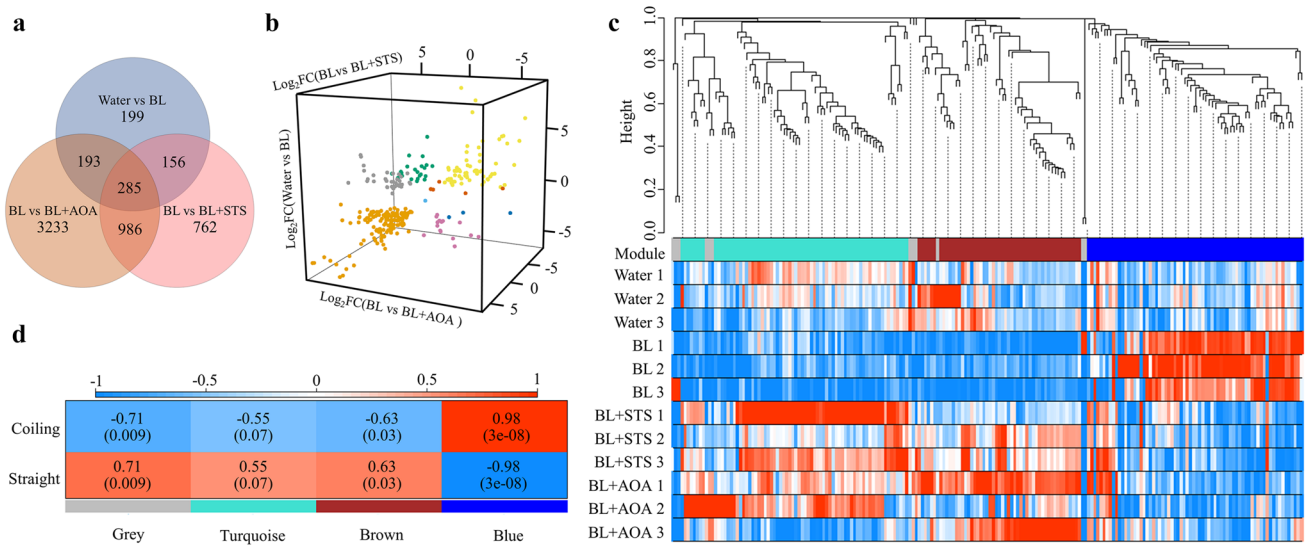

Fig. 2 Screening of DEGs and weighted gene co-expression network analysis (WGCNA). **a**Venn diagrams show the number of genes differentially expressed in Water versus BL, BL vs. BL + AOA, and BL versus BL + STS. The numbers in the overlapping areas indicate the number of shared genes; **b** Three-dimensional scatter plot shows the Log_2FC values of shared 285 DEGs in Water versus BL, BL versus BL + AOA, and BL versus BL + STS; **c** Hierarchical clustering tree (dendrogram) of 205 genes. The branches correspond to modules of highly interconnected genes. The color rows below the dendrograms indicate four gene modules; **d** Phenotypic correlations of four gene modules (blue, brown, turquoise, grey). The numbers in the heat map indicate phenotypic correlations and *P* values (in brackets)

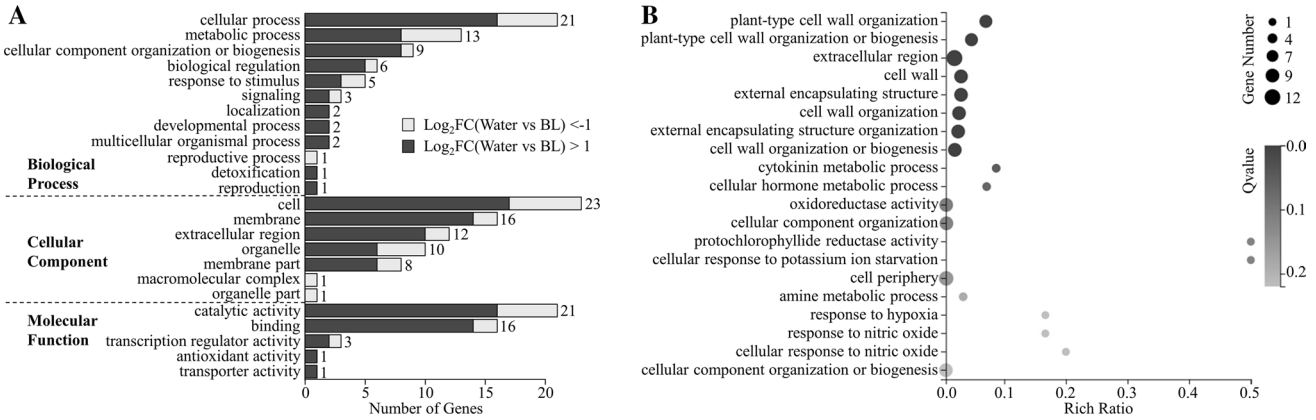

Fig. 3 Gene Ontology (GO) analysis. **a** GO classification. The number after each row refers to the amount of DEGs in different function groups. **b** GO enrichment. The Y-axis labels the enriched GO terms, and the X-axis labels the rich ratios of DEGs in different GO terms. The size of circles indicates the number of enriched genes, and the color depth indicates the *Q* value

"plant-type cell wall organization", "plant-type cell wall organization or biogenesis", "extracellular region", "cell wall", "external encapsulating structure", "cell wall organization", "external encapsulating structure organization", and "cell wall organization or biogenesis". Each of them included eight DEGs belonging to the *ALPHA-EXPANSIN* gene family (Table S8).

Co-expression Network Analysis of Module Genes

The co-expression network analysis of 70 DEGs in the blue module showed that the image obtained was composed of 70 nodes and 2048 edges (Table S9 and Table S10).

Based on the GO annotation, we focused on gene clusters with high GO enrichment degrees and large nodes,

meanwhile combined with The Arabidopsis Information Resource (https://www.arabidopsis.org), China Rice Data Center (http://www.ricedata.cn/gene/) and National Center for Biotechnology Information (https://www.ncbi.nlm.nih.gov/). Finally, we classified the 70 DEGs into six categories, containing "cell wall" (red nodes, 13), "oxidoreductases" (green nodes, 12), "binding" (blue nodes, 8), "metabolic process" (yellow nodes, 9), "cell membrane" (brown nodes, 6), and others (grey nodes, 22) (Fig. 4 and Table S10).

The DEGs in the "cell wall" were closely related to cell elongation and expansion. They mainly included 8 genes of *EXPA* family, namely *ALPHA-EXPANSIN 13* (*OsEXPA13*) (Os02g0267200), *ALPHA-EXPANSIN 14* (*OsEXPA14*) (Os02g0267700), *ALPHA-EXPANSIN 19* (*OsEXPA19*) (Os03g0156000), *ALPHA-EXPANSIN 20* (*OsEXPA20*) (Os03g0156300), *ALPHA-EXPANSIN 22* (*OsEXPA22*) (Os02g0268600), *Novel_G000182*, *Novel_G000183*, and *Novel_G000184*. Besides, there were *WALL-ASSOCIATED RECEPTOR KINASE-LIKE 16* (*OsWAKL16*) (Os09g0471200), *PECTIN ACETYLESTERASE 7* (*OsPAE7*) (Os04g060250), *PECTIN METHYLESTERASE 4* (*OsPME4*) (Os01g0634600), and *BASIC PATHOGENESIS-RELATED PROTEIN 1–2* (*OsPRB1-2*) (Os07g0128800).

The "oxidoreductases" were highly correlated with the synthesis of the endogenous hormone of plants. They mainly included 2 ETH synthase genes, namely *ACC oxidase 7* (*OsACO7*) (Os01g0580500) and its homologous gene *Novel_G000655*; 2 auxin synthase genes, namely *OsYUCCA6* (Os07g0437000) and *OsYUCCA8* (Os03g0162000); and a cytokinin-related gene, namely *CYTOKININ OXIDASE* (*OsCKX*) (Os01g0197600).

The "binding" had four transcription factor genes, which were *ETHYLENE-RESPONSIVE TRANSCRIPTION FACTOR 82*(*OsERF82*) (Os04g0399800), *ETHYLENE-RESPONSIVE TRANSCRIPTION FACTOR 60*(*OsERF60*) (Os03g0182800), *ETHYLENE-RESPONSIVE TRANSCRIPTION FACTOR 2*(*OsERF2*) (Os06g0181700), and *WUSCHEL RELATED HOMEOBOX 10* (*OsWOX10*) (Os08g0242400). Wherein *OsERF82*, *OsERF60*, and *OsERF2* belong to the *ERFs* family.

The "metabolic process" mainly included *CHITINASE 3* (*OsCHT3*) (Os06g0726100), *CHITINASE 1* (*OsCHT1*) (Os06g0726200), *LONELY GUY LIKE PHOSPHORIBOHYDROLASE 4* (*OsLOGL4*) (Os03g0697200), *TAU GLUTATHIONE S-TRANSFERASE 6* (*OsGSTU6*) (Os01g0558100), and *GLUCOSYL TRANSFERASE* (*UDP*)

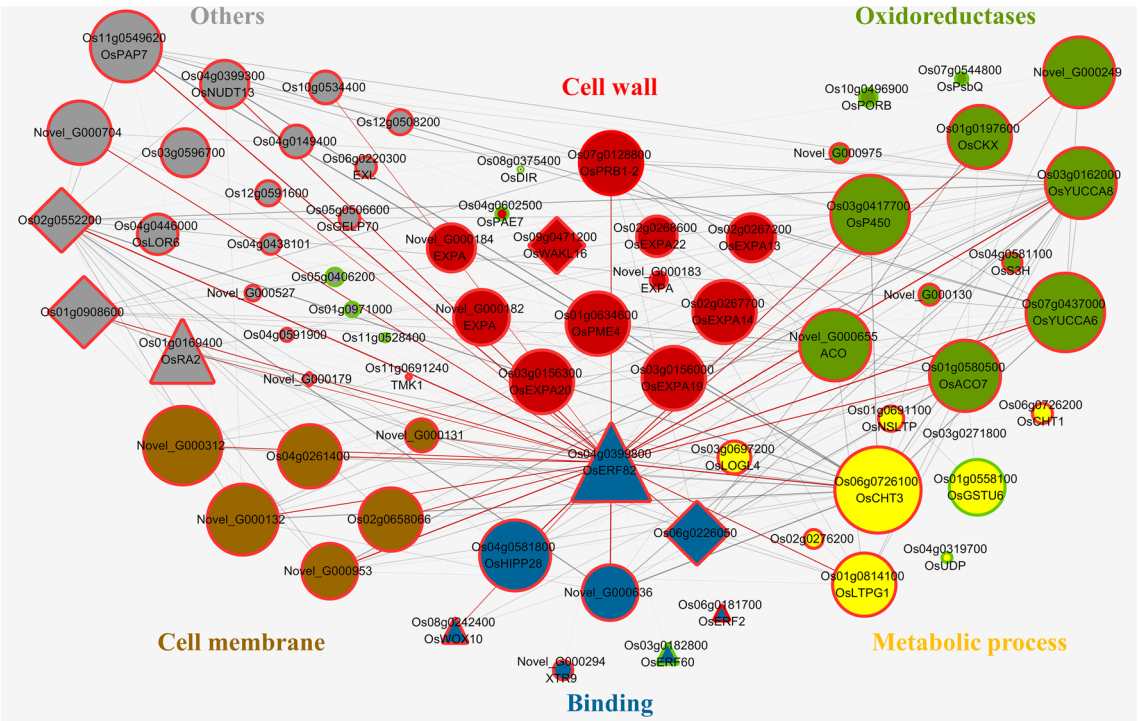

Fig. 4 Co-expression network of blue module genes. The nodes represent DEG. Node shapes are used to visualize the respective characteristics of DEG. Triangle represents transcription factor genes, the diamond represents receptor-like kinase genes, and the circle represents other genes. The red outer circle means that the DEG satisfies Log_2FC (Water vs. BL) > 1, log_2FC (BL vs. BL + AOA) < −1, and log_2FC (BL vs. BL + STS) < −1, simultaneously. The green outer circle means that the DEG satisfies Log_2FC (Water vs. BL) < −1, log_2FC (BL vs. BL + AOA) > 1, and log_2FC (BL vs. BL + STS) > 1, simultaneously. Different filling colors correspond to different types of genes. The thickness of lines represents the co-expression weight values between DEGs, in which the edges connected with *OsERF82* are outlined in red. For showing clearly, only the part with weight values ≥ 0.4 has been shown (Table S9)

(Os04g0319700), etc. Besides, the "cell membrane" mainly included 6 genes, such as Os02g0658066.

In the co-expression relationships, *OsERF82* connected to more nodes of DEGs in the above six categories. Besides, *OsERF82* was closely related to DEGs in the "oxidoreductases", especially *OsACO*s and *OsYUCCAs*, indicating that there was a prominent co-expression relationship between *OsERF82* and them. However, the relationship between *OsERF82* and DEGs in "cell wall" was comparatively weak, indicating no obviously direct regulation between them. What's more, the expressions of DEGs closely associated with *OsERF82* (weight ≥ 0.4) were all up-regulated in BL, which was dependent on ETH pathway.

Validation of RNA-Seq Data by qRT-PCR

We selected 12 genes and verified them by qRT-PCR. It has been reported that the receptor-like kinase (RLK) gene *ROOT MEADNDER CURLING* (*OsRMC*) inhibited root coiling. Meanwhile, in this study, the expression level of *OsRMC* was inhibited by BL. Finally, we picked out 12 genes, 5 of them involved in ETH pathway, 4 in cell elongation and expansion, 2 in auxin synthesis, and the *OsRMC*. The expressions trends in the above 12 genes were consistent with that of RNA-Seq data basically (Fig. 5; Table S11), reflecting the reliability of RNA-Seq data.

Discussion

The BR-induced ARG of *O. sativa* could be eliminated by ETH biosynthesis inhibitor (AOA) or perception antagonist (STS), indicating that the process depended on both ETH synthesis and signaling transduction (Cai et al. 2018). In *Arabidopsis*, when the concentration of exogenous BL was 10^{-8} M, the expression of *AtACO1* could be up-regulated (Park et al. 2019). Moreover, BL can promote ETH biosynthesis by improving the stability of ACS (Lee and Yoon 2018). In this study, the *OsACS2* and eight *OsACOs* were got by sequencing, in which the expression levels of *OsACS2* (Os04g0578000) and four *OsACOs* (Os01g0580500, Novel_G000655, Os11g0186900 and Os05g0149400, among which the first two were the DEGs in the blue module) were up-regulated by BL (Fig. S4 and Table S12). Besides, the expressions of 2 *OsERFs* (Os04g0399800 and Os06g0181700) in the blue module

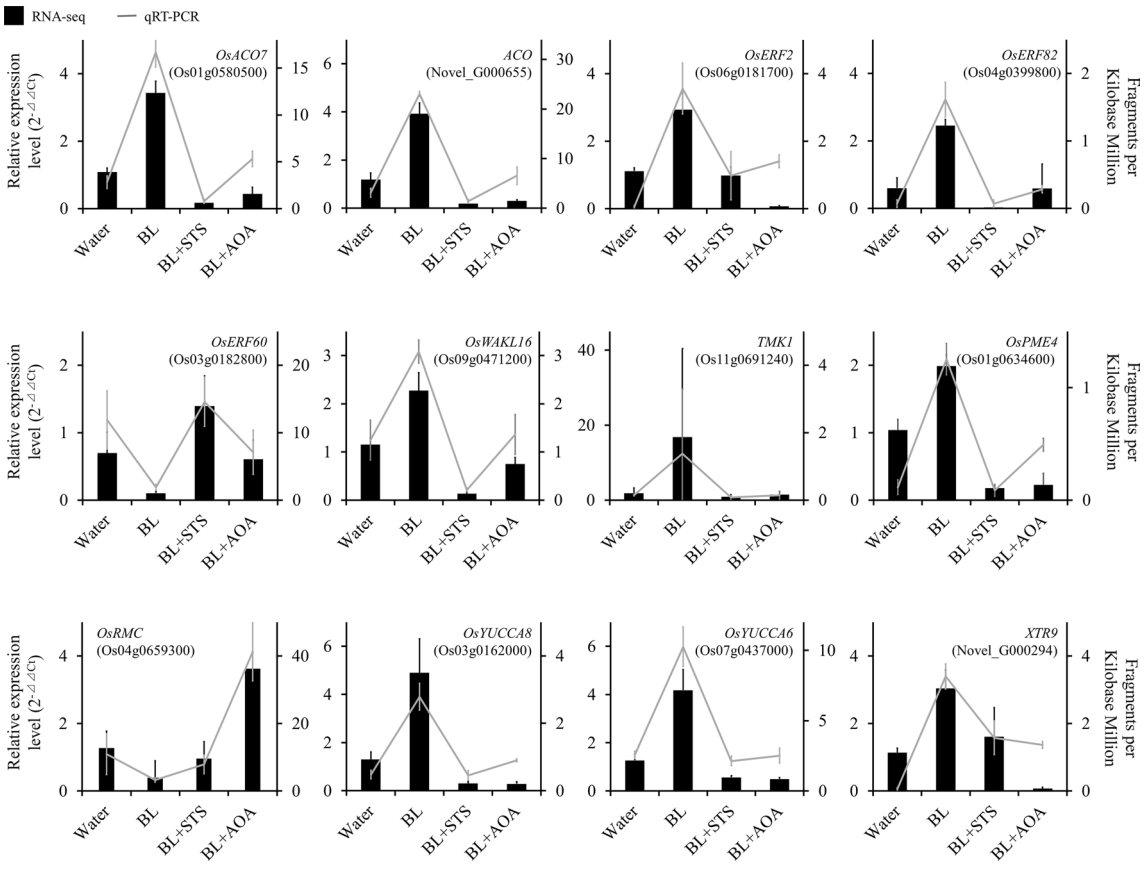

Fig. 5 Gene expression in RNA-seq and qRT-PCR. The results of RNA-seq and qRT-PCR of 12 genes are compared. The results of RNA-seq and qRT-PCR are shown by line charts and bar charts, respectively

were up-regulated by BL and down-regulated by ETH inhibitors. Therefore, on one hand, BRs might promote ETH synthesis and induce ARG by up-regulating the expression of *OsACOs* and *OsACS2*. However, whether the stability of ACSs could be enhanced in this process needs further verification. On the other hand, *OsERF82* may be an essential node for BL to induce ARG through ETH pathway and played a key role downstream of the ETH signaling pathway.

In the blue module, there were many DEGs regulating cell elongation, such as *OsEXPA*s, *OsWAK*, and *OsTMK*. As the α-subfamily of EXPANSIN, EXPAs can promote cell loose and elongation (Dongsu Choi et al. 2006).In the roots of *Vigna radiata* seedlings, the expressions of *OsEXPA*s increased with the increase of ETH concentrations (Huang et al. 2013). As Ser/Thr receptor kinases, WAKs could covalently bind to the pectin of cell wall components and regulate cell elongation (Lally et al. 2001; Decreux and Messiaen 2005). Besides, the transmembrane kinase TMKs subfamily of leucine-rich repeat (LRR) RLKs, specifically control cell elongation. In *Arabidopsis*, *TMKs* mutations lead to the short-root phenotype, while the number of cells unchanged (Beemster et al. 2013). Our previous research showed that in the concentration of 2×10^{-8} M BL, the inner and outer circle cells were elongated, but the outer circle cells were longer than the inner circle cells, resulting in the root coiling (Cai et al. 2018). In this study, expression levels of the above genes were all up-regulated by BL and down-regulated by ETH inhibitors, which indicated that BL could effectively regulate root elongation through ETH pathway. However, in the inner and outer circle cells of *O. sativa* primary roots, whether there are differences in the expression level of these genes needs further exploration.

The interactions of plant hormones in regulating ARG were complex, in which auxin played an important role (Roy and Bassham 2014). Exogenous application of ACC, the precursor of ETH, could significantly promote auxin synthesis in *Arabidopsis* roots (Swarup et al. 2007). In auxin synthesis, YUCCAs were key rate-limiting enzymes, and the expressions of *YUCCAs* could be up-regulated by BRs and ETH signalings in *Arabidopsis* roots (Vragović et al. 2015; Liu et al. 2016). In our study, the expressions of *OsYUCCAs* were also up-regulated in BRs, and this process was dependent on ETH pathway. Also, there were significant co-expression relationships between *OsERF82* and *OsYUCCA6*, as well as *OsYUCCA8*. Therefore, it could be speculated that there was a positive correlation between the up-regulated expressions of *YUCCAs* and the ARG phenotypes. In addition, it has been reported that the increase of auxin content can promote the acidification of the cell wall, and then activate EXPAs to enhance cell loose and elongation (McQueen-Mason et al. 1992). However, not only the auxin synthesis but also polar auxin transport was also important for ARG, so it is necessary to further study polar auxin transport in the future.

The RLK gene *OsRMC* is a negative regulator for the coiling process of root induced by JA. ERFs can bind to the *OsRMC* promoter region and regulate its expression (Jiang et al. 2007; Lourenço et al. 2015). In our study, the expression of *OsRMC* was down-regulated by BL and this process depended on ETH pathway. BRs could effectively inhibit the expression of *OsRMC* via ETH pathway to eliminate the restriction of *OsRMC* on ARG.

In conclusion, we have identified some genes related to the BR-induced ARG via ETH pathway at the transcriptional level and obtained 70 DEGs with high correlations and *OsRMC* that inhibited root coiling. On one hand, BL up-regulated the expression of at least two kinds of genes through ETH pathway, one was *OsEXPAs*, *OsWAK*, *OsTMK* that promote cell elongation; the other was plant hormone synthase genes, such as *OsACOs*, *OsYUCCAs*, *OsCKX*. With the function of the above genes, ARG was promoted. On the other hand, BL down-regulated the expression of *OsRMC* via ETH pathway, thus eliminating its restriction on ARG (Fig. S5). Of course, the functions of genes are not only at the transcriptional level but also the post-transcriptional level. Therefore, the functions of related genes should be further explored at the post-transcriptional level.

Supplementary Information The online version contains supplementary material available at https://doi.org/10.1007/s12374-021-09308-3.

Author contributions Conceptualization, ZC and JL; Funding acquisition, JL, ZC and XY; Investigation, ZC, ZH, CH, XJ, WY, GJ, and FW; Project administration, ZC; Resources, JL, ZC and XY. Visualization, ZC, ZH, CH, and ZW; Validation, ZC; Writing—original draft, ZC, ZH and CH; Writing—review and editing, ZC and ZH. All authors have read and agreed to the published version of the manuscript.

Funding This work was supported by Hainan Provincial Natural Science Foundation of China [320RC508], Hainan Provincial Natural Science Foundation of China [319MS017], Hainan University Scientific Research Startup Fund Project [kyqd1620], and Innovation and entrepreneurship training program for college students [SA2000008501].

Availability of data and materials The transcriptome sequencing data has been submitted to the SRA database of NCBI with the accession number of SRP278550.

Code availability Not applicable.

Declarations

Conflicts of interest The authors declare no conflict of interest.

Ethics approval Not applicable.

Consent to Participate The authors declare consent to participate.

Consent for Publication The authors declare consent for publication.

References

Bajguz A (2007) Metabolism of brassinosteroids in plants. Plant Physiol Biochem 45:95–107. https://doi.org/10.1016/j.plaphy.2007.01.002

Beemster GTS, Dai N, Wang W, Patterson SE, Bleecker AB (2013) The TMK subfamily of receptor-like kinases in *Arabidopsis* display an essential role in growth and a reduced sensitivity to auxin. PLoS ONE 8:e60990. https://doi.org/10.1371/journal.pone.0060990

Beyer EM (1976) A potent inhibitor of ethylene action in plants. Plant Physiol 58:268–271. https://doi.org/10.1104/pp.58.3.268

Beyer EM (1979) Effect of silver ion, carbon dioxide, and oxygen on ethylene action and metabolism. Plant Physiol 63:169–173. https://doi.org/10.1104/pp.63.1.169

Blancaflor EB, Masson PH (2003) Plant gravitropism. Unraveling the ups and downs of a complex process. Plant Physiol 133(4):1677–1690. https://doi.org/10.1104/pp.103.032169

Buer CS, Wasteneys GO, Masle J (2003) Ethylene modulates root-wave responses in *Arabidopsis*. Plant Physiol 132(2):1085–1096. https://doi.org/10.1104/pp.102.019182

Cai ZP, Yang W, Zhang HY, Luo JJ, Wu FH, Jing X, Meng SL, Wang XY, Yu XD (2018) Ethylene participates in the brassinolide-regulated asymmetric growth of *O sativa* root. S Afr J Bot 119:86–93. https://doi.org/10.1016/j.sajb.2018.08.017

Cao L, Fu Y, Yu XD, Cai ZP, Luo JJ, Tang Z, Huang XW (2019) Brassinosteroid induces asymmetric growth of primary roots in *Brassica chinensis L.* Chin J Trop Crops 40:468–474. https://doi.org/10.3969/j.issn.1000-2561.2019.03.008

Choi D, Cho H-T, Lee Y (2006) Expansins: expanding importance in plant growth and development. Physiol Plant 126:511–518. https://doi.org/10.1111/j.1399-3054.2005.00612.x

Clouse SD, Langford M, McMorris TC (1996) A brassinosteroid-insensitive mutant in *Arabidopsis* thaliana exhibits multiple defects in growth and development. Plant Physiol 111(3):671–678. https://doi.org/10.1104/pp.111.3.671

Darwin C (1880) The power of movements in plants. John Murray, London

Decreux A, Messiaen J (2005) Wall-associated kinase WAK1 interacts with cell wall pectins in a calcium-induced conformation. Plant Cell Physiol 46:268–278. https://doi.org/10.1093/pcp/pci026

Fridman Y, Elkouby L, Holland N, Vragović K, Elbaum R, Savaldi-Goldstein S (2014) Root growth is modulated by differential hormonal sensitivity in neighboring cells. Genes Dev 28:912–920. https://doi.org/10.1101/gad.239335.114

Fujioka S, Li J, Choi Y-H, Seto H, Takatsuto S, Noguchi T, Watanabe T, Kuriyama H, Yokota T, Chory J, Sakurai A (1997) The *Arabidopsis* deetiolated2 mutant is blocked early in brassinosteroid biosynthesis. Plant Cell 1997(9):1951–1962. https://doi.org/10.1105/tpc.9.11.1951

Gudesblat GE, Russinova E (2011) Plants grow on brassinosteroids. Curr Opin Plant Biol 14:530–537. https://doi.org/10.1016/j.pbi.2011.05.004

Yueqing H, Shitou X, Yi S, Huiqun W, Weigui L, Shengying S, Langtao X (2016) Brassinolide increases potato root growth in vitro in a dose-dependent way and alleviates salinity stress. BioMed Res Int. https://doi.org/10.1155/2016/8231873

Huang W-N, Liu H-K, Zhang H-H, Chen Z, Guo Y-D, Kang Y-F (2013) Ethylene-induced changes in lignification and cell wall-degrading enzymes in the roots of mungbean (*Vigna radiata*) sprouts. Plant Physiol Biochem 73:412–419. https://doi.org/10.1016/j.plaphy.2013.10.020

Jiang J, Li J, Xu Y, Han YE, Bai YUE, Zhou G, Lou Y, Xu Z, Chong K (2007) RNAi knockdown of *Oryza sativa root meander curling* gene led to altered root development and coiling which were mediated by jasmonic acid signalling in rice. Plant Cell Environ 30:690–699. https://doi.org/10.1111/j.1365-3040.2007.01663.x

Kohl M, Wiese S, Warscheid B (2011) Cytoscape: software for visualization and analysis of biological networks. Methods Mol Biol 696:291–303. https://doi.org/10.1007/978-1-60761-987-1_18

Kurepin LV, Bey MA, Back TG et al (2016) Structure-Function Relationships of Four Stereoisomers of a Brassinolide Mimetic on Hypocotyl and Root Elongation of the Brassinosteroid-Deficient *det2-1* Mutant of *Arabidopsis*. J Plant Growth Regul 35:215–221. https://doi.org/10.1007/s00344-015-9523-8

Lally D, Ingmire P, Tong H-Y, He Z-H (2001) Antisense expression of a cell wall-associated protein kinase, WAK4, inhibits cell elongation and alters morphology. Plant Cell 13:1317–1332. https://doi.org/10.1105/tpc.13.6.1317

Langfelder P, Horvath S (2008) WGCNA: an R package for weighted correlation network analysis. BMC Bioinform 9:559. https://doi.org/10.1186/1471-2105-9-559

Lanza M, García-Ponce B, Castrillo G, Catarecha P, Sauer M, Rodríguez M, Paez A, Sánchez-Bermejo E, Mohan TC, Puerto Y, Sandalio L, Paz-Ares J, Leyva A (2012) Role of actin cytoskeleton in brassinosteroid signaling and in its integration with the auxin response in plants. Dev Cell 22:1275–1285. https://doi.org/10.1016/j.devcel.2012.04.008

Lee HY, Yoon GM (2018) Regulation of ethylene biosynthesis by phytohormones in etiolated rice (*Oryza sativa L.*) Seedlings. Mol Cells 41:311–319. https://doi.org/10.14348/molcells.2018.2224

Jianming L, Kyoung N (2002) Regulation of brassinosteroid signaling by GSK3/SHAGGY-like kinase. Science 295:1299–1301. https://doi.org/10.1126/science.1065769

Liu G, Gao S, Tian H, Wu W, Robert HS, Ding Z (2016) Local transcriptional control of *YUCCA* regulates auxin promoted root-growth inhibition in response to aluminium stress in *Arabidopsis*. PLoS Genet 12(10):e1006360. https://doi.org/10.1371/journal.pgen.1006360

Lourenço TF, Serra TS, Cordeiro AM, Swanson SJ, Gilroy S, Saibo NJM, Oliveira MM (2015) The rice E3-Ubiquitin ligase HIGH EXPRESSION OF OSMOTICALLY RESPONSIVE GENE1 modulates the expression of *ROOT MEANDER CURLING* a gene Involved in root mechanosensing, through the interaction with two ETHYLENE-RESPONSE FACTOR transcription factors. Plant Physiol 169:2275–2287. https://doi.org/10.1104/pp.15.01131

Mandava NB (1988) Plant growth-promoting brassinosteroids. Annu Rev Plant Physiol Plant Mol Biol 39:23–52. https://doi.org/10.1146/annurev.pp.39.060188.000323

McQueen-Mason S, Durachkoand DM, Cosgrove DJ (1992) Two endogenous proteins that induce cell wall extension in plants. Plant Cell 4(11):1425–1433. https://doi.org/10.1105/tpc.4.11.1425

Migliaccio F, Piconese S (2001) Spiralizations and tropisms in *Arabidopsis* roots. Trends Plant Sci 6:561–565. https://doi.org/10.1016/s1360-1385(01)02152-5

Mori A, Toyota M, Shimada M, Mekata M, Kurata T, Tasaka M, Morita MT (2016) Isolation of new gravitropic mutants under hypergravity conditions. Front Plant Sci 7:01443. https://doi.org/10.3389/fpls.2016.01443

Nymeijer K, Visser T, Brilman W, Wessling M (2004) Analysis of the complexation reaction between Ag^+ and ethylene. Ind Eng Chem Res 43:2627–2635. https://doi.org/10.1021/ie0341350

Okada K, Shimura Y (1990) Reversible root tip rotation in *Arabidopsis* seedlings induced by obstacle-touching stimulus. Science 250(4978):274–276. https://doi.org/10.1126/science.250.4978.274

Park C-H, Seo C, Park YJ, Youn J-H, Roh J, Moon J, Kim S-K (2019) BES1 directly binds to the promoter of the ACC oxidase 1 gene to

regulate gravitropic response in the roots of *Arabidopsis thaliana*. Plant Signal Behav 15:1690724. https://doi.org/10.1080/15592324.2019.1690724

Peiser GD, Wang TT, Hoffman NE, Yang SF, Liu HW, Walsh CT (1984) Formation of cyanide from carbon 1 of 1-aminocyclopropane-1-carboxylic acid during its conversion to ethylene. Proc Natl Acad Sci U S A 81:3059–3063. https://doi.org/10.1073/pnas.81.10.3059

Pfaffl MW (2001) A new mathematical model for relative quantification in real-time RT-PCR. Nucleic Acids Res 29:45. https://doi.org/10.1093/nar/29.9.e45

Robert HS, Friml J (2009) Auxin and other signals on the move in plants. Nat Chem Biol 5(5):325–332. https://doi.org/10.1038/nchembio.170

Roy R, Bassham DC (2014) Root growth movements: waving and skewing. Plant Sci 42–47:0168–9452. https://doi.org/10.1016/j.plantsci.2014.01.007

Spollen WG, LeNoble ME, Samuels TD, Bernstein N, Sharp RE (2000) Abscisic acid accumulation maintains maize primary poot elongation at low water potentials by restricting ethylene production. Plant Physiol 122:967–976. https://doi.org/10.1104/pp.122.3.967

Swarup R, Perry P, Hagenbeek D, Van Der Straeten D, Beemster G, Sandberg G, Bhalerao R, Ljung K, Bennett M (2007) Ethylene upregulates auxin biosynthesis in *Arabidopsis* seedlings to enhance inhibition of root cell elongation. Plant Cell 19:2186–2196. https://doi.org/10.1105/tpc.107.052100

Tanveer M, Shahzad B, Sharma A, Biju S, Bhardwaj R (2018) 24-Epibrassinolide; an active brassinolide and its role in salt stress tolerance in plants: A review. Plant Physiol Biochem 130:69–79. https://doi.org/10.1016/j.plaphy.2018.06.035

Vragović K, Sela A, Friedlander-Shani L et al (2015) Translatome analyses capture of opposing tissue-specific brassinosteroid signals orchestrating root meristem differentiation. Proc Natl Acad Sci USA 112(3):923–928. https://doi.org/10.1073/pnas.1417947112

Wang H, Liang X, Wan Q, Wang X, Bi Y (2009) Ethylene and nitric oxide are involved in maintaining ion homeostasis in *Arabidopsis* callus under salt stress. Planta 230:293–307. https://doi.org/10.1007/s00425-009-0946-y

Wang L, Feng Z, Wang X, Wang X, Zhang X (2010) DEGseq: an R package for identifying differentially expressed genes from RNA-seq data. Bioinformatics 26:136–138. https://doi.org/10.1093/bioinformatics/btp612

Woods SL, Roberts JA, Taylor IB (1984) Ethylene-induced root coiling in tomato seedlings. Plant Growth Regul 2:217–225. https://doi.org/10.1007/bf00124770